Polymer Spot Size Expanders for High Efficiency Optical Coupling in Optical Interconnection

Yoshiki Kamiura,[*1] Taiga Kurisawa,[1] Chiemi Fujikawa,[1] and Osamu Mikami[2]

[1] *Course of Electrical and Electronic Engineering, Graduate School of Engineering, Tokai University, 4-4-1, Kitakaname, Hiratsuka, Kanagawa, 259-1292, Japan*
[2] *Malaysia-Japan International Institute of Technology, Universiti Teknologi Malaysia, 54100 Jalan Sultan Yahya Petra, Kuala Lumpur, Malaysia*

Received August 03, 2022; accepted September 29, 2022; published September 30, 2022

Abstract—Improving low coupling efficiency due to spot size differences between silicon photonics chips and single mode fibers remains a challenge for achieving high bit-rate optical interconnections. To solve this problem, a test spot size expander device is fabricated using UV-curable resin on the end face of the fiber with a high numerical aperture having a similar spot size of silicon chips. The expanded spot size of 9.38 μm from the original 3.2 μm at a wavelength of 1.55 μm and the maximum coupling efficiency with a single mode fiber of –1.19 dB is achieved. In addition, the –3 dB tolerance of the coupling efficiency along the vertical optical axis was ±4.1 μm.

Recently, silicon photonics technology has attracted considerable attention because of the growing need for high-bit-rate optical interconnections. However, the low optical coupling efficiency between silicon photonic (SiPh) chips and single-mode optical fibers (SMFs) remains a challenge. The spot size of the SiPh chip is typically enlarged to 3–4 μm from the submicrons by a spot size converter (SSC) integrated in the SiPh chip. The low efficiency, particularly in the edge coupling scheme, is primarily due to the difference in the spot size of the SiPh chips (3–4 μm) and that of SMFs (10 μm) [1]. To overcome this problem, researchers have produced coupling devices fabricated on the end face of an SMF [2–5]. In addition, the connection of SMF and SiPh using a tapered self-written waveguide has been proposed [6–8]. The precise adjustment of two spot sizes within a few submicrons is extremely difficult, particularly in the fiber implementation stage. Recently, attempts have been made to integrate a silicon waveguide with a special structure, such as a 3D bending mirror, within a SiPh chip [9, 10]. The fabrication of these integrated structures requires extremely sophisticated silicon-processing techniques.

In this study, a unique spot size expander (SSE) was proposed to expand the spot size from 3 μm to 10 μm for the first time. The SSE was fabricated using only UV-curable resin via self-written waveguide technology [11] and/or the photomask transfer method [12]. This fabrication method is simple, inexpensive, and does not require expensive processing equipments. A test sample was designed and fabricated with UV-cured resin on the facet of 3–4 μm high numerical aperture (HiNA) fibers instead of an SiPh chip [13]. It is because, unfortunately, the valuable SiPh chip is not very easy to obtain in a university lab. The HiNA fiber has a similar small spot size to the SiPh chip. In the following the detail of designing of the proposed SSE is described. Then optical characteristics, coupling efficiency and –3 dB tolerance of the coupling efficiency of the fabricated SSE are reported.

The fundamental structure of the proposed device is shown schematically in Fig. 1. An SSE composed of a pillar and microlens was fabricated on the end of the HiNA fiber. To ensure that the SSE and HiNA fiber aligned precisely in the submicron order, the pillar was fabricated using a conventional, precisely controlled photomask aligning process, and the microlens was fabricated on the pillar by a dipping process [14].

The output spot size ($2\omega_0$) of the SiPh chip was converted to a spot size of $2\omega_2$ (a diameter of 10 μm) to efficiently couple the optical device and SMF during the ordinary fiber attachment stage. The expanded spot size was expected to mitigate the tolerance vertical to the optical axis.

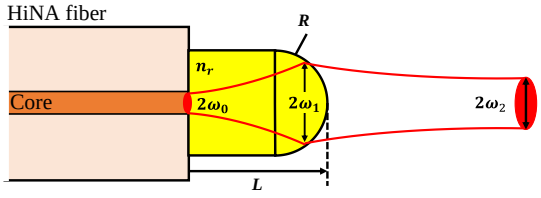

Fig. 1. Proposed SSE structure. The optical beam ($2\omega_0$) from the SSC is expanded within the SSE; subsequently, the microlens converts the spot diameter to a ($2\omega_2$) of 10 μm.

Subsequently, the optimal shape of the SSE was calculated. Assuming that the SSE height and refractive

* E-mail: 1ceim015@mail.u-tokai.ac.jp

index of the microlens are L and n_r, respectively, the wavelength of the signal is $\lambda = 1.55$ µm.

Furthermore, assuming a Gaussian beam, the beam radius ω_1 is enlarged as follows [15].

$$\omega_1 = \omega_0 \sqrt{1 + \left(\frac{\lambda L}{\pi n_r \omega_0^2}\right)^2} \quad (1)$$

where ω_0 is the output spot size of the SSC. The beam diameter $2\omega_1$ was enlarged to over 30 µm for the SSE with a height L of 90 µm.

The wavefront of the Gaussian beam was converted using the convex lens effect of the microlens. The spot size $2\omega_2$ and spot position Z were calculated as a function of the radius of curvature R of the microlens, as follows [15].

$$\omega_2 = \frac{\omega_0}{\sqrt{\left(\frac{\pi\omega_0}{\lambda}\right)^2 \left(\frac{n_r - n_a}{n_a}\frac{1}{R}\right)^2 + \left(1 + \frac{n_a - n_r}{n_r}\frac{L}{R}\right)^2}} \quad (2)$$

The calculated $2\omega_2$ and Z values are shown in Fig. 2, where the SSE height L, was set to 90 µm. For example, a spot size ($2\omega_2$) of 10 µm was achieved when $R = 25$ µm and $Z = 164$ µm.

The proposed SSE was fabricated using UV-curable resin ("SUNCONNECT," Nissan Chemical Corporation) [16] and a self-written waveguide method [11, 12]. The SSE was fabricated on the end of a HiNA fiber, UHNA7, NUFERN having a similar mode field diameter (MFD) as the conventional SSC of the SiPh chip. The data sheet of UHNA7 indicates that the cladding diameter is 125.0 ± 1.5 µm, the core diameter is 2.4 µm, the MFD is approximately 3.2 ± 0.3 µm at a wavelength of 1.55 µm, and the NA is 0.41 [17–18].

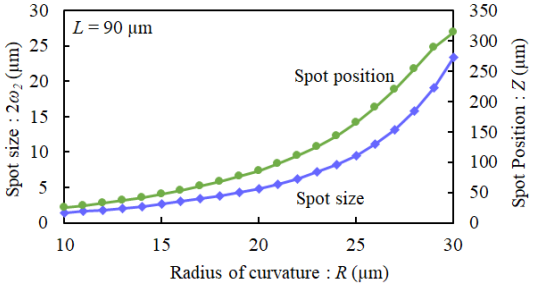

Fig. 2. Beam diameter $2\omega_1$ as a function of the SSE height L of the microlens.

The fabrication process of the pillars and microlenses is illustrated in Fig. 3. A multimode fiber with a core size of 50 µm was used because it was much simpler than using the photomask as a preliminary stage. First, an MMF with a core diameter of 50 µm and a HiNA fiber were precisely aligned using a 1.55 µm laser beam as the monitoring signal. The end face of the MMF was subjected to anti-sticking treatment. The MMF and HiNA fibers were shifted according to the pre-designed gap value, and the gap was filled with resin. Second, the resin was cured by irradiation with a 405-nm laser light from the MMF side. The irradiation time was 15 s with an optical output power of approximately 180 µW. Subsequently, the uncured parts were cleaned. Next, a microlens was fabricated on the pillar using the dipping method. The dipping method is convenient for fabricating microlenses in a limited area [14]. The diameter of the microlens fabricated on the end face of the pillar depends on the diameter of the pillar. The edge of the pillar was slowly placed on a thin coating of resin on a glass slide. When the edge of the pillar came into contact with the resin, it was quickly pulled off the glass slide. Subsequently, the resin attached to the pillar top was cured using an LED with a wavelength of 365 nm. Finally, the uncured parts were cleaned.

A scanning electron microscopy (SEM) image of the fabricated SSE is shown in Fig. 4(a). The SSE has a height L of 89.2 µm, a diameter of 46.9 µm for the microlens and pillar, and a thickness of 19.3 µm for the microlens. Assuming that the microlens shape is approximated as a sphere, the radius of curvature R was calculated as 23.9 µm. This value was estimated from the thickness and diameter of the microlens as measured with SEM.

The optical properties of the SSE were evaluated using near-field pattern (NFP) measurements. The NFP for the SSE output beam at the 1.55 µm wavelength is shown in Fig. 4(b). The spot size was determined from the $1/e^2$ intensity distribution of the peak value. The spot size of the SSE was expanded to 9.38 µm for the HiNA fiber.

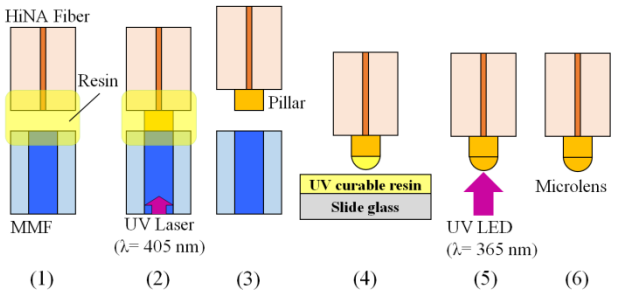

Fig. 3. Fabrication process of the pillar and the microlens.

The optical coupling efficiency of the SSE was measured using the setup shown in Fig. 5. The beam with the wavelength of 1.55 µm emitted from the HiNA fiber with the SSE was received by an SMF with an MFD of 10.4 µm at a wavelength of 1.55 µm [17]. The optical coupling efficiency between the HiNA fiber with SSE and SMF is shown in Fig. 6. The theoretical optical coupling efficiency was calculated for the SSE with a height (L) of 90 µm and radius of curvature (R) of 25 µm. A maximum coupling efficiency of –1.19 dB was obtained from the

experiment. In contrast, the butt coupling efficiency between the SMF and HiNA fiber was –3.55 dB.

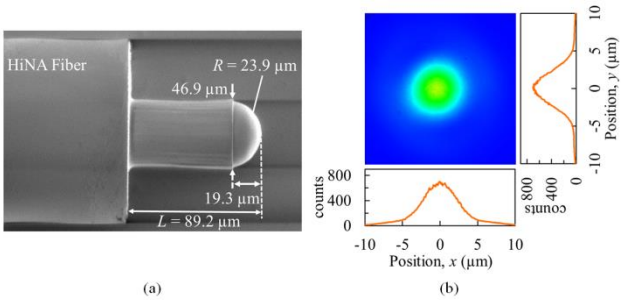

Fig. 4. SEM photograph of fabricated the SSE (a) and near field pattern at 1.55 µm wavelength (b). Beam emitted from the HiNA fiber is expanded to approximately 10 µm.

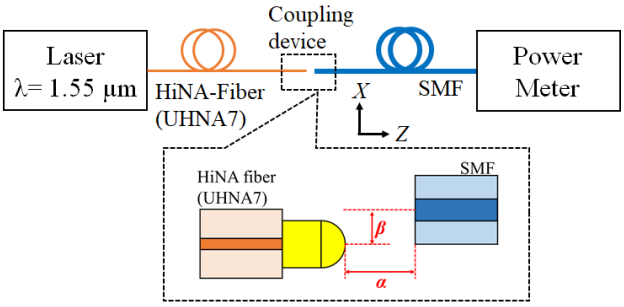

Fig. 5. Measurement setup for coupling efficiency between HiNA fiber and SMF.

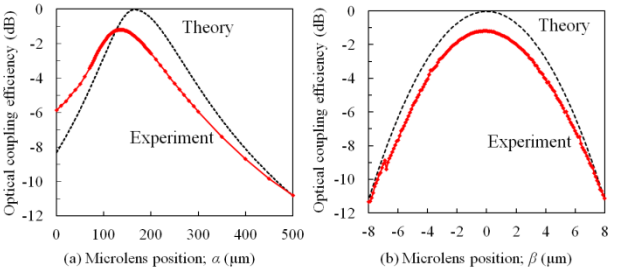

Fig. 6. Measured and theoretical coupling efficiency and positional tolerance. (a) Displacement parallel to the optical axis of fiber; *Z* and (b) Vertical displacement to the optical axis of fiber; *X*

This maximum value was observed at a position far from the SMF end face, as shown in Fig. 6(a). This is a typical characteristic of SSE. The difference between theory and experiment with respect to the optimum microlens position may be due to the safety gap which was included to prevent physical contact with the device. In addition, the –3 dB tolerance of the coupling efficiency along the vertical optical axis was ±4.1 µm, as shown in Fig. 6 (b). As expected, the spot size expanded by the SSE mitigated the tolerance in the direction vertical to the optical axis of the fiber.

In conclusion, a SSE coupling device consisting of a pillar and a microlens on the HiNA fiber was proposed. This device increases the spot size as expected and eases the tolerance in the both directions perpendicular and parallel to the optical axis.

Presently, the miniaturization of the SSE is under consideration, and the fabrication of a new SSE on the end-face of a real SiPh chip is under preparation.

This work was supported in part by A-STEP (Adaptable and Seamless Technology Transfer Program through Target-driven R&D), JPMJTM20DA of JST (Japan Science and Technology). We thank Nissan Chemical Corporation for providing the UV-curable resin.

References

[1] R. Marchetti, C. Lacava, L. Carroll, K. Gradkowski, P. Minzioni, Photonics Research, **7**(2), 201 (2019).
[2] R. Bachelot, C. Ecoffet, D. Deloeil, P. Royer, D.J. Lougnot, App. Opt. **40**(32), 5860 (2001).
[3] L. Xiao, W. Jin, M.S. Demokan, H.L. Ho, H.Y. Tam, J. Ju, J. Yu, Opt. Lett. **31**(12), 1791 (2006).
[4] O. Mikami, R. Sato, S. Suzuki, C. Fujikawa, IEEE Photonics Technol. Lett. **32**(7), 399 (2020).
[5] Y. Kamiura, T. Kurisawa, C. Fujikawa, O. Mikami, Jpn. J. Appl. Phys. **61** SK1009, (2022).
[6] T. Kurisawa, Y. Kamiura, C. Fujikawa, O. Mikami, Proc. 2021 IEEE CPMT Symposium Japan (ICSJ), pp. 102-103, (2021).
[7] H. Terasawa, O. Sugihara, J. Lightwave Tech. **39**(23), 7472 (2021).
[8] Y. Saito, K. Shikama, T. Tsuchizawa, N. Sato, Opt. Lett. **47**(12), 2971 (2022).
[9] A. Noriki, I. Tamai, Y. Ibusuki, A. Ukita, S. Suda, D. Shimura, Y. Onawa, H. Yaegashi, T. Amano, J. Lightwave Tech. **38**(12), 3147 (2020).
[10] T. Amano, A. Noriki, I. Tamai, Y. Ibusuki, A. Ukita, S. Suda, T. Kurosu, K. Takemura, T. Aoki, D. Shimura, Y. Onawa, H. Yaegashi, OFC2021, Th4A.1, (2021).
[11] S.J. Frisken, Opt. Lett. **18**(13), 1035 (1993).
[12] Y. Obata, Y. Oyama, H. Ozawa, T. Ito, O. Mikami, T. Uchida, ICEP2005, pp. 225-229, April 2005.
[13] Y. Kamiura, T. Kurisawa, C. Fujikawa, O. Mikami, Proc. 2021 IEEE CPMT Symposium Japan (ICSJ), pp. 104-105 (2021).
[14] N.A. Baharudin, C. Fujikawa, O. Mikami, S.M. Idrus, S. Ambran, Jpn. J. Appl. Phys. 58, SJJB02 (2019).
[15] K. Kawano, Appl. Opt. **25**(15), 2600 (1986).
[16] H. Nawata, K. Ohmori, Proc. International Conference on Electronics Packaging (ICEP), Toyama, Japan, Apr. 23-25, (2014).
[17] P. Yin, J.R. Serafini, Z. Su, R.-J. Shiue, E. Timurdogan, M.L. Fanto, S. Preble, Opt. Expr. **27**(17), 24188 (2019).
[18] https://coherentinc.force.com/Coherent/UHNA7?cclcl=en_US, (12/09/2022).

